"Physics of Auroral Phenomena", Proc. XLII Annual Seminar, Apatity, pp. 107-110, 2019

Polar Geophysical Institute

DOI: 10.25702/KSC.2588-0039.2019.42.107-110

COMPARISON OF THE DIURNAL VARIATIONS OF THE BOTTOM EDGE OF THE IONOSPHERE DURING TWO PROTON PRECIPITATIONS ON AND AFTER 29 SEPTEMBER 1989, 19 OCTOBER 1989

M.I. Sukhovey[2], V.A. Shishaev[1], G.F. Remenets[2]

[1]*Polar Geophysical Institute, Apatity, Russia*
[2]*Saint-Petersburg State University, Saint-Petersburg, Russia*

Abstract. The purpose of our work is to get the solutions of the inverse VLF problems during the powerful solar proton precipitations (SPP), which continued several days and began on September 29, 1989, 1200 UT [1, 2], and October 19, 1989, 1300 UT [1]. We compared quantitatively the daily variations of the solar proton fluxes with the dynamics of the reflection properties of the bottom edge of the ionosphere. For this realization, we used the variations of VLF signals for a completely auroral VLF propagation path Aldra (Northern Norway) – Apatity (Kola Peninsula).

Introduction. Application of VLF sounding for calculation of the D-region dynamics was made possible by the usage of ground-based VLF system which consisted of a transmitter located on island Aldra, Northern Norway, $66.7°N$ 13.1° and a receiver located in Apatity, Kola Peninsula, $67.6°N$ $33.4°E$. This VLF propagation path had a length equal to 885 km. The phase and amplitude variations of three signals $(i = 1,2,3; f_1 = 10.2kHz, f_2 = 12.1kHz, f_3 = 13.6kHz)$were recorded at the Polar Geophysical Institute, RAS. The examples of these records are shown in Figs. 1 and 2.

During SPP, protons with energy less than 10 MeV has a relatively small contribution in ionization at the heights below 60 km [3]. The proton fluxes used by us were measured onboard the GOES 6 satellite in integral channels $(> 1MeV, > 5MeV, > 10MeV, > 30MeV, > 50MeV, > 60MeV, > 100MeV)$ [1], and they were referred to two multiday SPP. First SPP began on September 29 at 1205 UT [1, 2, 4] (X-ray flare 1047 UT X9.8 [4]). On September 30, its flux with the energy $E > 10\ MeV$ had a maximum mean value $F_{E>10MeV} = 10^3 cm^{-2}s^{-1}sr^{-1}$ for 4 hours of the VLF propagation path sunset. Second SPP began on October 19, 1305 UT (X-ray flare 1229 UT X13.0 / 4B [5]), proton flux had a maximum $F_{E>10MeV} = 20 \cdot 10^3 cm^{-2}s^{-1}sr^{-1}$ on October 20. This event was characterized with a sharp increase of the flux with the maximum value $F_{E>10MeV} = 10^3 cm^{-2}s^{-1}sr^{-1}$ on October 22, id. est. this value was 20 times weaker than the previous maximum.

The dynamics of the reflection properties of the lower ionosphere (D-region) is described by us as the time functions of the complex reflection coefficient. This coefficient was found with the help of the self-consistent method used for the solution of an inverse VLF problem [2, 6] in which the input data are presented as a set of 3 amplitude (in relative units) and 3 phase variations (in microseconds), Figs. 1 and 2. In this method the output data are two variations: a reflection coefficient modulus of the first hop (1-st ray) $R(t)$ and the effective height $h(t)$ of the terrestrial waveguide, Figs. 3 and 4. The initial values $h_0,\ R_0$ of the parameters are not known to us. For this reason, we calculate all feasible solutions with different $h_0,\ R_0$. From all of these possible solutions, we take one that minimizes a discrepancy function $G(h_0,\ R_0)$ [2, 6]. This function uses the differences between the input experimental data $E_i(t_n),\ \varphi_i(t_n)$ and the calculated ones $\tilde{E}_i(t_n),\ \tilde{\varphi}_i(t_n)$:

$$G(h_0,\ R_0) = \sum_{i=1}^{3}\sum_{n=1}^{m}\left[\frac{[\tilde{E}_i(t_n)-E_i(t_n)]^2}{E_i^2(t_0)} + \frac{[\tilde{\varphi}_i(t_n)-\varphi_i(t_n)]^2}{\Delta\varphi_i^2}\right],$$

where the first term in the brackets presents the difference between calculated and experimental amplitude time functions which are normalized in such a way that $\tilde{E}_i(t_0) = E_i(t_0)$. The t_0 is the initial time of a disturbance. The second term presents the difference between calculated and experimental phase time functions, which are such that $\tilde{\varphi}_i(t_0) = \varphi_i(t_0)$ and which are divided on the maximal variation of the phase for a frequency with a number i. The m is a number of time steps for the disturbance.

The results and discussion. The solutions that minimize the discrepancy function $G(h_0,\ R_0)$ for each sunset are shown in Figs. 3 and 4. In these figures the $h(t)$ and $R(t)$ variations for both SPP are presented as functions of solar zenith angle for four days: the day before the beginning of SPP (quiet conditions) and three days after the beginning of it (disturbed conditions). Having these quantitative results of the inverse problem solution we consider in Table 1 the variations of effective height h_{day} under day conditions (zenith angle of the Sun is $\chi < 92°$ at the middle point of the VLF propagation path) and effective height h_{night} under night conditions (zenith angle of the Sun is $\chi > 98°$ at the middle point of the VLF propagation path). According to this table, in particular, a sunset change of the effective height before the first SPP in September was from 64 to 78 km and the same change before the second SPP in October was from 63 to 70 km. The most interesting result, which is seen from the Table 1 and Figs. 3 and 4, is the fact that in the cases of both SPP the dependences of $h(t)$ and $R(t)$ on solar zenith angle became significantly weaker but did not disappear [7], although these solar proton precipitations are the ones of the strongest.

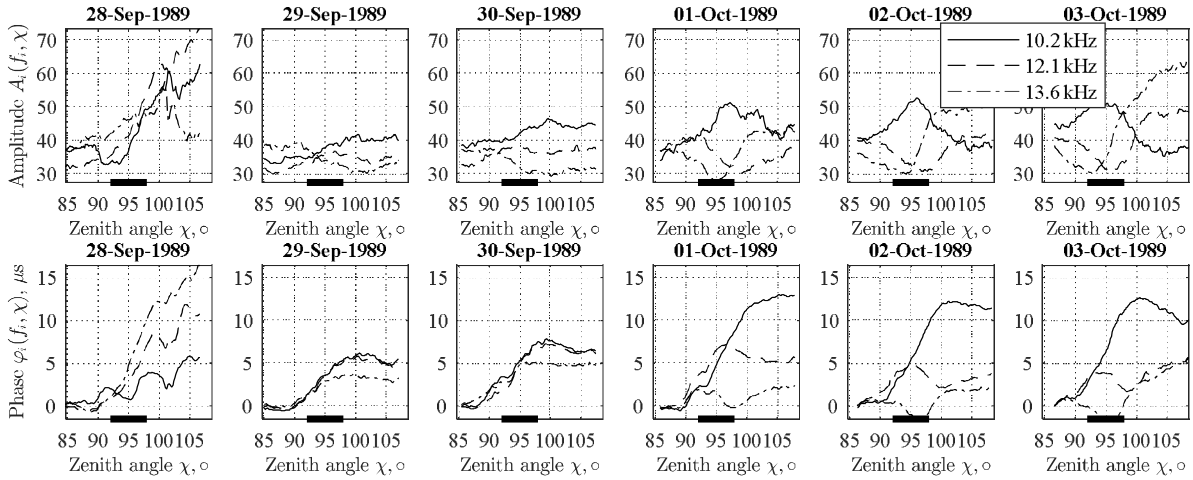

Figure 1. Experimental amplitude (*top row*) and phase (*bottom row*) variations of the three signals which propagated along the radio path Aldra – Apatity (time step was 100 sec). SPP began on September 29 at 1205 UT. Each subgraph displays a day-to-night transition process, it implies a zenith angle of the Sun was $92° < \chi < 98°$ (as indicated by the black horizontal bar). The left column shows variations on September 28 when the conditions were quiet. Other columns demonstrate the first five days after the beginning of the SPP (September 29, 30 and October 1-3).

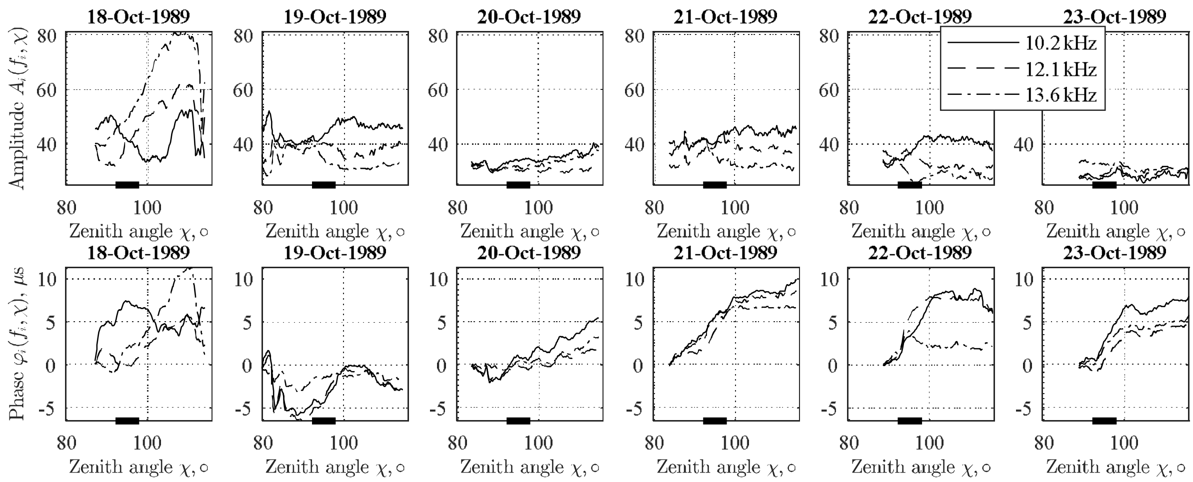

Figure 2. This figure is the same as the previous one, but for the second SPP which began on October 19 at 1300 UT. The left column shows variations on October 18 when the conditions were quiet. Other columns represent the first five days after the beginning of the SPP (October 19-23).

Among the solutions we choose those that had the closest flux values $F_{E>10MeV}$ from both events: for the first event, on October 1, the effective height changed from $h_{day} = 53\,km$ to $h_{night} = 63\,km$ while the proton flux was $F_{E>10MeV} = 70\,cm^{-2}s^{-1}sr^{-1}$; for the next event on October 19 and 22 the effective height values changed from $h_{day} = 52\, and\, 51\,km$ to $h_{night} = 56\, and\, 58\,km$, while the proton fluxes were $F_{E>10MeV} = 100$ and $70\,cm^{-2}s^{-1}sr^{-1}$, respectively. This comparison would seem to suggest that for the second SPP the proton flux rigidity significantly greater (for electrical conductivity below 60 km) than for the first one.

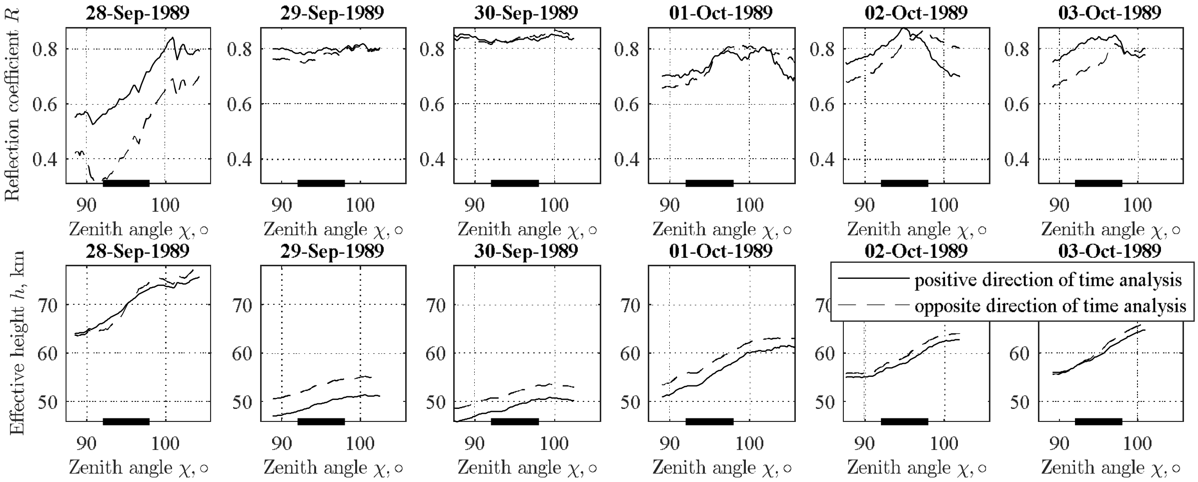

Figure 3. Reflection coefficient modulus R (*top row*) and effective height h (*bottom row*) as functions of solar zenith angle. The inverse problem was solved independently for natural (solid line) and reversed (dashed line) time sequences. The SPP began on September 29. The left column shows variations on September 28 when the conditions were quiet. Other columns represent the first five days after the beginning of the SPP (September 29, 30 and October 1-3).

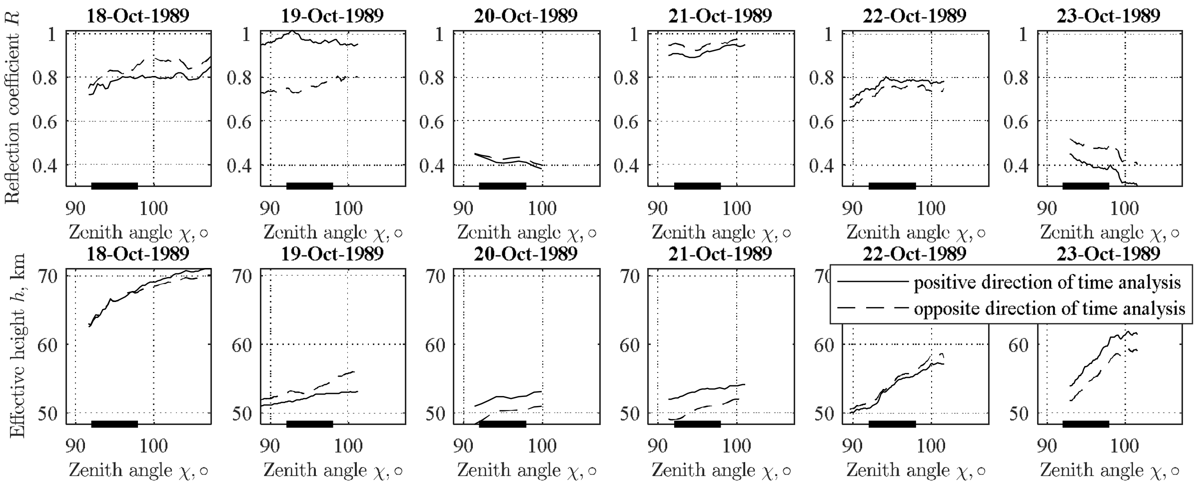

Figure 4. This figure is the same as the previous one, but for the second SPP which began on October 19 at 1300 UT. The left column shows variations on October 18 when the conditions were quiet. Other columns demonstrate the first five days after the beginning of the SPP (October 18 - 23).

Repeated X-ray flare (on 23 October, X2.9, 1708 UT [5]) was accompanied by increased proton flux. This flux with $E > 10\ MeV$ was almost similar with the flux of the beginning of the first event (September 29): the effective height changed from 51 to 55 km for the proton fluxes $F_{E>10MeV} = 900\ cm^{-2}s^{-1}sr^{-1}$, on September 29 and it changed from 52 to 59 km for the proton flux $F_{E>10MeV} = 1000\ cm^{-2}s^{-1}sr^{-1}$ on October 23. Accordingly, the day-to-night variations of effective height were $\Delta h = 4$ and 7 km. These values indicate that the repeated SPP on October 23 had lower proton flux rigidity than it was at the beginning of the first event on September 29. This conclusion is consistent with the solar proton flux values with the energy $E > 100\ MeV$, which were $F_{E>100MeV} = 300$ and 50 $cm^{-2}s^{-1}sr^{-1}$, respectively. Before this analysis, we were able to suggest that in these events there was full "locking" of the electromagnetic waves in the terrestrial waveguide between the ground surface and the bottom fringe of the ionosphere disturbed. Because of the effect pointed, we see that in reality, the electromagnetic waves penetrate to the heights of the ionospheric D-layer which was controlled by the solar zenith angle [7].

Conclusions. With the help of the ground-based VLF method [2, 7], the dynamics of the reflection coefficient R modulus and effective height h were investigated for two SPP events on September 29, 1989, and October 19, 1989. This analysis made it possible to compare the electron conductivity properties of the lower fringe of the ionosphere for these two events. We have shown that both SPP begun under quiet conditions, namely effective height values under day conditions were $h_{day} = 64$ and $63\ km$ and under night conditions these values were $h_{night} = 78$ and $70\ km$. Because of the activity of auroral electrons with energy less than $300\ KeV$, the night values differ. It is important to note that when proton flux values were maximal for both events (on September 30 and October 20) effective height variations were 4 and $3\ km$, respectively. Despite the presence of the strong source of ionization, namely precipitated protons with fluxes values up to $F_{E>10MeV} = 20 \cdot 10^3\ cm^{-2}s^{-1}sr^{-1}$, diurnal variations of the electron conductivity became significantly weaker but did not disappear. This effect means that the VLF signal variations were caused by sunset solar zenith angle changes although one might have expected an absence of such dependence. Therefore, in spite of the intensive ionization of atmosphere below $60\ km$ by the solar proton precipitations, the electromagnetic waves in both events reached the altitudes of the regular ionospheric D-layer, which disappeared at night.

Table 1. The values of effective height h and reflection coefficient modulus R under night and day conditions. In the left part of the table, these parameters are shown for undisturbed conditions (September 28) and the following disturbed days. In the right part of the table, the analogous data are presented for the second event; October 18 was an undisturbed day.

SPP on and after 29 Sep 1989						SPP on and after 19 Oct 1989					
Date	Day conditions		Night conditions		$F_{>10MeV}$, $cm^{-2}s^{-1}sr^{-1}$	Date	Day conditions		Night conditions		$F_{>10MeV}$, $cm^{-2}s^{-1}sr^{-1}$
	h, km	R	h, km	R			h, km	R	h, km	R	
28 Sep.	64	0.4	78	0.7	0.1	18 Oct.	63	0.75	70	0.9	0.1
29 Sep.	51	0.75	55	0.8	900	19 Oct.	52	0.75	56	0.8	100
30 Sep.	49	0.85	53	0.85	1000	20 Oct.	48	0.45	51	0.4	20000
1 Oct.	53	0.65	63	0.75	70	21 Oct.	49	0.95	52	0.95	400
2 Oct.	56	0.7	64	0.8	20	22 Oct.	51	0.65	58	0.75	70
3 Oct.	56	0.75	65	0.8	9	23 Oct.	52	0.5	59	0.4	1000

References

1. National Center for Environmental Information
2. *https://satdat.ngdc.noaa.gov/sem/240goes/data/avg/1989/09/goes06/csv/*
3. Remenets, G.F., M.I. Beloglazov. Dynamics of an auroral ionospheric fringe at geophysical disturbances on 29 September 1989 // Planet. Space Sci. 1992. V. 40. P. 1101-1108.
4. Bailey, D.K. Abnormal ionization in the lower ionosphere associated with cosmic-ray flux enhancements, Proc. IRE. 1959. 47. 255.
5. Coffey, H.E. Solar-Geophysical Data Number 542, October 1989. Part 1 (prompt reports). Data for September, August 1989, and Late Data, p. 25, 42. United States: 1989. Web.
6. Coffey, H.E. Solar-Geophysical Data Number 543, November 1989. Part 1 (prompt reports). Data for October, September, 1989, and Late Data, p.25,39-41. United States: N. p., 1989. Web.
7. Remenets, G. F., M. I. Beloglazov. An initial analysis of the dynamics of reflection properties of the low ionosphere at dawn for an auroral radio pass (according to the VLF data). Geomagn. Aeronom. 1985. V. 25. P. 69-72. (In Russian).
8. Remenets, G. F., M. I. Suhovey, V. A. Shishaev. Sunset variations of the bottom edge of the ionosphere during the proton precipitations on and after 29 September 1989, Springer Proc. In Earth and Environmental Sciences, Problems of Geocosmos–2018. Proc. XII Int. Con. and School. p. 319-332. 2020.